Published in final edited form as:
Dev Dyn. 2009 September ; 238(9): 2318–2326. doi:10.1002/dvdy.21886.

The *Flk1-myr::mCherry* mouse as a useful reporter to characterize multiple aspects of ocular blood vessel development and disease

Ross A. Poché[1], **Irina V. Larina**[1], **Melissa L. Scott**[2], **Jennifer E. Saik**[3], **Jennifer L. West**[3], and **Mary E. Dickinson**[1,2,*]

[1]Department of Molecular Physiology and Biophysics, Baylor College of Medicine, Houston, TX 77030, USA.

[2]Program in Developmental Biology, Baylor College of Medicine, Houston, TX 77030, USA.

[3]Department of Bioengineering, Rice University, Houston, TX 77005, USA.

Abstract

The highly vascularized mouse eye is an excellent model system in which to elucidate the molecular genetic basis of blood vessel development and disease. However, the analysis of ocular vessel defects has traditionally been derived from fixed tissue which fails to account for dynamic events such as blood flow and cell migration. To overcome the limitations of static analysis, tremendous advances in imaging technology and fluorescent protein reporter mouse lines now enable the direct visualization of developing cells *in vivo*. Here, we demonstrate that the *Flk1-myr::mCherry* transgenic mouse is an extremely useful live reporter with broad applicability to retinal, hyaloid and choroid vascular research.

Keywords

eye; endothelial cells; blood vessels; retina; hyaloid; choroid

INTRODUCTION

As in other body tissues, the eye requires a complex vascular system which provides oxygen, nutrients, waste removal and promotes homeostasis. The eye contains three vascular beds, the transient hyaloid vasculature, the retinal vessels and the choroidal vessels (Saint-Geniez and D'Amore, 2004). The hyaloid vessels, an arterial network, support the embryonic growth of the eye and initially extend from the optic nerve into the vitreous where they wrap around the developing lens. Ultimately, via a macrophage mediated response, the hyaloid vessels undergo apoptosis (Lang and Bishop, 1993; Lang et al., 1994). In the mouse, hyaloid degeneration occurs during early postnatal stages and since the hyaloid's pupillary membrane covers the anterior surface of the lens, it is possible to directly image vessel apoptosis (Meeson et al., 1996; Ritter et al., 2005).

Retinal vessels, composed of both arteries and veins, begin to develop postnatally as the hyaloid system is regressing (Saint-Geniez and D'Amore, 2004; Fruttiger, 2007). From postnatal day 0 to 7, the primary retinal vascular plexus develops on the retinal surface, in a

[*]**Author for correspondence:** Mary E. Dickinson, Associate Professor, Department of Molecular Physiology and Biophysics, MS335, Baylor College of Medicine, mdickins@bcm.edu, Telephone: 713-798-2104, Fax: 713-798-3475.

central to peripheral fashion, with vessels located at the vascular front being less mature than vessels near the optic nerve. By postnatal day 18, the primary vasculature has infiltrated the inner retinal layers thereby forming the intermediate and deep capillary beds within the inner and outer plexiform layers, respectively (Fruttiger, 2007). Since the retinal vasculature develops with such a specific temporal and spatial order and is easily examined in flat mounts, it has become a popular model system to investigate molecular pathways regulating vessel development.

The choroidal vessel network is derived from vasculature that extends from the developing neural tube and encircles the outer layer of the optic cup. This system ultimately forms a highly fenestrated capillary bed located between the sclera and the retinal pigment epithelium and provides support to the avascular outer retinal layers, including the photoreceptors (Campochiaro and Hackett, 2003; Saint-Geniez and D'Amore, 2004).

In addition to being a valuable system for addressing fundamental questions regarding blood vessel development, the eye is susceptible to significant vascular pathologies associated with several diseases (Saint-Geniez and D'Amore, 2004; Friedlander, 2007). Patients suffering from age-related macular degeneration (ARMD) exhibit vessel outgrowth from the choroid into the subretinal space often resulting in fluid accumulation. This can lead to retinal or retinal pigment epithelium detachment and central vision loss. ARMD is the primary cause of blindness of individuals over 65 years of age living in industrialized nations (Klein et al., 1992; Saint-Geniez and D'Amore, 2004). If the hyaloid vessels fail to regress, a condition known as hyperplastic primary vitreous develops and is associated with intraocular hemorrhage, retinal detachment and cataracts (Goldberg, 1997).

Multiple pathologies are associated with retinal vessel neovascularization as a response to a hypoxic retinal environment. These include retinopathy of prematurity (ROP), proliferative diabetic retinopathy and venous occlusion (Saint-Geniez and D'Amore, 2004; Gariano and Gardner, 2005; Fruttiger, 2007). The normally avascular cornea is also susceptible to pathological neovascularization which can significantly hinder vision. This condition is normally secondary to corneal insults such as persistent hypoxia, infection or chemical exposure and is also a complication affecting successful corneal transplants (Panda et al., 2007).

In recent years, mouse gene targeting and transgenesis have begun to unravel molecular pathways essential for proper vessel development and much progress has been made toward addressing the mechanisms underlying vascular disease. However, most of these studies have been performed on fixed tissue, which do not give a full representation of the dynamic nature of this system. To reveal dynamic events associated with development and disease, researchers are beginning to use live imaging of the mouse eye (Ritter et al., 2005; Speier et al., 2008). In this paper, we report the ocular expression of the recently developed *Flk1-myr::mCherry* transgenic mouse which exhibits endothelial cell-specific expression of a myristoylated mCherry fluorescent protein (Larina et al., in press). Our data show that this line will be of great use to those wishing to perform static as well as *in vivo* imaging of ocular vessel dynamics.

In order to demonstrate the utility of this reporter line, we performed *ex vivo* and *in vivo* imaging of three separate eye vascular systems over time (summarized in Fig. 1A–C). Specifically, we characterized Flk1-myr::mCherry localization in the degenerating pupillary membrane (PM) of the hyaloid vascualture, in the developing retina and in VEGF-induced corneal neovascularization. We found *Flk1-myr::mCherry* mice exhibit robust expression in all ocular vessel beds and that the myristoylation of the mCherry protein results in efficient labeling of the membrane, providing reliable information about endothelial cell structure.

In vivo confocal imaging revealed that the *Flk1-myr::mCherry* transgene robustly labels the degenerating hyaloid vasculature. Moreover, since the myr::mCherry protein is tethered to the cell membrane, we were able to detect myr::mCherry-labeled cellular debris engulfed by macrophages which are implicated in hyaloid vessel regression (Lang and Bishop, 1993). Additionally, since mCherry is spectrally distinct from Green Fluorescent Protein (GFP), the *Flk1-myr::mCherry* line can be crossed with a GFP-expressing line, such as the ε*-globin-KGFP* line (Dyer et al., 2001) to enable live imaging of vessel morphology and blood flow simultaneously. In the developing retina, myr::mCherry labeled the earliest stages of vessel sprouting from the optic nerve head (ONH). Extensive membrane sprouting and projection toward the retinal periphery were observed throughout the entire period of retinal development. We failed to detect myr::mCherry+ endothelial precursor cells seeded within the retina ahead of the vascular front (McLeod et al., 2006; Hasegawa et al., 2008). These data are consistent with an angiogenic rather than a vasculogenic mode of retinal vessel development. Finally, we employed the corneal micropocket assay to show that the *Flk1-myr::mCherry* reporter labels adult neovessels induced by angiogenic growth factors and provides a useful reagent for those attempting to understand and treat corneal neovascularization.

RESULTS AND DISCUSSION

Flk1-myr::mCherry Expression in the Regressing Hyaloid Vasculature *in vivo*

In order to define the expression of the *Flk1-myr::mCherry* mouse for performing *in vivo* imaging of vascular systems, we performed short-term, live imaging of the postnatal PM at multiple time points. At P0, a brightly labeled, dense network of PM blood vessels was observed (Fig. 1A). At later time points, 3, 7 and 10 days postnatally, we observed the characteristic progressive regression of the PM while the peripheral vessels within the iris persist (Fig. 2B–D) (Ito and Yoshioka, 1999). By P16, the entire PM area was avascular (data not shown). Interestingly, when imaging these mice under high magnification, we consistently observed myr::mCherry+ puncta within the PM vascular field (Fig. 2E–H, arrows). We presumed these structures were cellular debris derived from apoptotic PM endothelial cells. In order to confirm this, we made fixed PM flat mounts from P4 mice and performed immunofluorescence with an antibody against F4/80. This antibody has been used extensively to label resident PM macrophages (Lobov et al., 2005). At low magnification, we observed F4/80+ macrophages throughout the PM vasculature network and not the iris (Fig. 3A and B). Higher magnification images of the region shown in Fig. 3A shows close association of macrophages with the regressing myr::mCherry+ vasculature. In our confocal images, we were able to resolve isolated myr::mCherry+ puncta and observed that they are always localized within F4/80+ macrophages (Fig. 3C–F, arrowheads). Thus, Flk1-myr::mCherry, by virtue of being a plasma membrane-linked fluorescent protein, efficiently labels EC debris being engulfed by macrophages. In total, these data suggest that the *Flk1-myr::mCherry* mouse is a useful live imaging reagent for revealing novel aspects of vessel apoptosis *in vivo*.

Live Imaging of Postnatal Vessel Blood Flow

One benefit of generating this line with mCherry is that it is spectrally distinct from many other fluorescent proteins such as GFP (Shaner et al., 2005). This enables spectral separation of GFP and mCherry using conventional filters and allows for simultaneous imaging of both markers. To demonstrate this, we crossed *Flk1-myr::mCherry* mice with ε*-globin-KGFP*$^{+/tg}$ mice (Dyer et al., 2001) and we used high-speed confocal microscopy to image the vessels in the pupillary membrane and iris (not shown) of P0 *Flk1-myr::mCherry*$^{+/tg}$; ε*-globin-KGFP*$^{+/tg}$ mice (Fig. 4A–C and Supplemental movies 1 and 2). GFP+ blood cells (Fig. 4A) were easily distinguished from the mCherry marker in the surrounding vessels (Fig. 4B) and

could be easily tracked using automated analysis (Imaris software package, Bitplane Inc) (Fig. 4C and Supplemental movies 1 and 2). Using the Imaris software, blood cells are identified by the GFP signal, individual positive cells are labeled with white spheres and tracks are represented by colored lines in which the color of an individual track changes over time (Fig. 4C). The signal from both markers was acquired simultaneously, permitting us to image rapidly enough to detect continuous tracks of fast moving blood cells within myr::mCherry-labeled vessels.. Thus, the eyes of *Flk1-myr::mCherry*$^{+/tg}$; ε*-globin-KGFP*$^{+/tg}$ mice can be used as an accessible model system in which to study the role of hemodynamics on postnatal vessel biology.

Flk1-myr::mCherry Labels All Stages of Retinal Vessel Development

By generating fixed retinal flat mounts, we characterized *Flk1-myr::mCherry* retinal expression from the time of vessel genesis to full differentiation (Fig 5 A). At P0, thin endothelial cell projections were seen entering the retina through the optic nerve head (ONH) (Fig. 5B). Two days later, these vessels progressed further toward the retinal periphery and began to exhibit more blood vessel-like morphologies (Fig. 5C). We were also able to detect discrete endothelial cell branching (Fig. 5D, arrow). By P7, distinct arterial and venous differentiation was observed (Fig. 5E) and the vascular front had almost extended to the retinal periphery (Fig. 5F). At P15, by generating a three-dimensional Z-stack through the entire thickness of the retina, we observed a mature primary vascular network as well as deeper vessel branches projecting into the retinal plexiform layers (Fig. 5G, I and Supplemental Movie 3). Figure 5H highlights the difference in depth of individual vessels by using the depth coding function in the Zeiss LSM 510 software. The three-dimensional Z-stack projection is color coded from the most superficial, primary plexus (red) to the deeper plexuses (blue) (Fig. 5H). These data show that the *Flk1-myr::mCherry* mouse is a useful reporter for characterizing retinal vessel morphology.

Flk1-myr::mCherry Expression is Consistent with an Angiogenic Model of Retinal Vessel Development

There has been an ongoing debate in the field as to whether vertebrate retinal blood vessels develop via angiogenesis (proliferation and sprouting of pre-existing vessels) or vasculogenesis (*de novo* differentiation of endothelial precursor cells into vessels) (Dorrell et al., 2002; Fruttiger, 2002; McLeod et al., 2006; Fruttiger, 2007; Hasegawa et al., 2008). It is well established that retinal vessels originate at the ONH and spread over the inner retinal surface from a central to peripheral fashion. Preceding the vascular front is a network of astrocytes which the vessels appear to use as a template for development. At P0, before the upregulation of the astrocyte marker GFAP, spindle-shaped cells are observed ahead of the vessel network (Chan-Ling et al., 1990; Fruttiger, 2002). It has been proposed that these cells are angioblasts seeded within the retina ahead of the vascular front thereby providing a means for vasculogenesis (Reveiwed in Fruttiger, 2002; Gariano, 2003). Vegf receptor-2 (Flk1) is an early marker of endothelial cell precursors (Millauer et al., 1993; Yamaguchi et al., 1993). Thus, if retinal vascularization occurs via vasculogenesis, we would expect to observe Flk1-myr::mCherry+ EC precursors ahead of the vascular network forming vessels *de novo*. By examining fixed retinal flat mounts, no such cell types were observed (Fig. 6A, arrowhead). Instead, we observed extensive branching of pre-existing myr::mCherry+ vessels (Fig. 6D, arrows). Moreover, by labeling the retinae with an antibody against astroglial-expressed transcription factor Sox2, we detected Sox2+, spindle-shaped cells well ahead of the myr::mCherry+ vessels (Fig. 6B–C, arrows) (Komitova and Eriksson, 2004; Bani-Yaghoub et al., 2006). At P4, Sox2+ cells co-labeled with GFAP thereby confirming their identity as astrocytes (data not shown). The specificity of the Sox2 marker was further demonstrated by analyzing the DAPI+ nuclei of myr::Cherry+ vessels and Sox2+ astrocytes.

Here, all nuclei belonging to the vessels were negative for Sox2 expression (Fig. 6E, arrows).

These data, while not conclusive, are consistent with the idea that retinal vessel development is an angiogenic process. Nevertheless, despite the fact that we observed *Flk1-myr::mCherry* fluorescence in the E7.5 blood islands (Larina et al., in press), it is still possible that the *Flk1-myr::mCherry* transgene does not contain all the necessary regulatory elements or expresses at sufficient levels to be detected in all early endothelial cell progenitors. Thus, an undetected resident population of retinal angioblasts may still exist.

Flk1-myr::mCherry is Useful for High-resolution, Long-term Imaging of Induced Neovascularization

For efficient transmittance and refraction of light, the cornea has evolved as an avascular tissue (Ambati et al., 2006; Beebe, 2008). Nevertheless, despite its normally avascular nature, the cornea is still capable of experiencing substantial neovascularization in response to severe physical, chemical, and thermal injury, implantation of tumors and other physiological insults (Langham, 1953; Gimbrone et al., 1973; Gimbrone et al., 1974; Muthukkaruppan and Auerbach, 1979). The cornea micropocket assay has capitalized upon this property and is often considered the gold-standard to determine whether signaling peptides, drugs, etc. function as pro-angiogenic or anti-angiogenic factors *in vivo* (Kenyon et al., 1996; Rogers et al., 2007). The method entails making a partial thickness incision into the mouse corneal stroma and inserting a slow-releasing polymer pellet, such as hydron, containing the candidate angiogenic factor. Over time, the mouse is monitored as limbic vessels enter the cornea and extend toward the pellet. We wanted to determine if adult corneal neovessels would express Flk1-myr::mCherry. Since hydron is no longer commercially available, we instead used Vascular endothelial growth factor (VEGF)-releasing hydrogels to induce angiogenesis. This method induced corneal neovascularization with the same general temporal and spatial characteristics as published reports using VEGF-releasing hydron pellets (Kenyon et al., 1996; Rogers et al., 2007). Indeed, by analyzing corneal flat mounts 6 days post-gel implantation, we observed an extensive network of myr::mCherry+ vessels (Fig. 7A–D). Some of these vessels contained RBCs suggesting the formation of patent vessels that are continuous with the circulation (Fig. 7E–G). Thus, the *Flk1-myr::mCherry* mice are useful for high resolution monitoring of corneal neovessel morphology induced by a variety of experimental factors and drug treatments.

In summary, the *Flk1-myr::mCherry* transgenic mouse is an excellent model for studying multiple aspects of eye vessel biology. In addition to its utility as an *in vivo* reporter for hyaloid vessel regression and corneal neovascularization, this line can be crossed into different mutants to label and study aberrant ocular development and disease. Additionally, the bright endothelial fluorescence will facilitate fluorescence-activated cell sorting (FACS) of endothelial cells which would allow for gene profiling experiments.

EXPERIMENTAL PROCEDURES

Mouse Strains

ε-*globin-KGFP*$^{tg/tg}$ mice (Dyer et al., 2001) were maintained on a CD1 background and *Flk1-myr::mCherry*$^{tg/tg}$ mice (Larina et al., in press) were maintained on both a mixed FVB/CD1 and FVB/C57BL/6J background. For all retinal expression studies, *Flk1-myr::mCherry*$^{+/tg}$ mice were PCR genotyped for the absence of the *retinal degeneration (rd)* allele using previous published conditions (Gimenez and Montoliu, 2001).

Microscopic Imaging

Imaging of fluorescent reporters was performed using either the Zeiss LSM 5 LIVE or the Zeiss LSM 510 META inverted microscope systems (Carl Zeiss Inc.). Flk1-myr::mCherry was excited using either a 543 nm laser (LSM 510 META) or a 532 nm laser (LSM 5 LIVE) and images obtained at different magnifications ranging from 10X to 63X. ε-globin-KGFP was excited with a 488 nm laser on both microscopes. For *in vivo* imaging of postnatal pupillary membrane vessels, neonates were sedated via isoflurane inhalation and a small incision was made through the eyelid in order to expose the eye. The eye was topically anesthetized with one drop of 0.5% proparacaine (Bausch and Lomb). If pupil dilation was needed, one drop of 1% tropicamide (Bausch and Lomb) was applied. The animal was immediately positioned on a glass coverslip with its eye parallel to the glass surface and secured to the stage of an inverted Zeiss LSM 5 LIVE microscope equipped with a homemade environmental chamber maintained at 37°C. Before sedation, a ring of molding clay was pressed against the bottom of the glass coverslip and filled with Viscotear solution (Novartis). The clay ring was used as a means to prevent the eye from directly contacting the glass coverslip and the Viscotear solution was used to prevent drying of the eye. Live imaging of ε-globin-KGFP+ blood flow through the Flk1-myr::mCherry+ pupillary membrane vessels was performed at 30 frames per second (fps). Immediately after imaging, the sedated animals were sacrificed via decapitation. The objectives used for specific imaging experiments are indicated in the figure legends.

Tissue Processing and Immunofluorescence

Eyes from *Flk1-myr::mCherry* mice were enucleated and fixed in 4% paraformaldehyde (PFA) for up to 1 hour at 4° C. The tissue was then washed in 1X phosphate-buffered saline (PBS, pH 7.3) and subsequently dissected into retinal, corneal or pupillary membrane flat mounts. For immunofluorescence, the mounted tissue was then washed in 1X PBS-T (PBS + 0.1% Triton X-100) 3 times at room temperature and blocked for 1 hour in a solution of 2% Bovine Serum Albumin (BSA) in PBS-T. Primary antibodies were diluted in the same blocking solution and incubated on the tissue overnight at 4° C in a humid chamber. The next day, the tissue was washed 4 times at room temperature in 1X PBS-T. Labeling with the secondary antibodies was performed using the same blocking solution (2% normal serum in 1X PBS-T) and samples incubated for 1 hour at room temperature. This was followed by staining with 4’,6-diamidino-2-phenylindole (DAPI) and mounting on glass slides using fluoromount-G (SouthernBiotech). All double-labeling experiments were performed by mixing primary antibodies followed by labeling with a mixture of the corresponding secondary antibodies. All secondary antibodies were Alexa Fluor-conjugated antibodies from Molecular Probes (Eugene, OR) and used at a dilution of 1:400. The primary antibodies used were goat anti-Sox2 (1:100, Santa Cruz sc-17320), rat anti-F4/80 (1:100, Invitrogen MF48000) and rabbit anti-GFAP (1:200, DAKO Z0334).

Preparation of VEGF-releasing hydrogels

Hydron slow-release polymer is normally used in the corneal micropocket assay but is no longer commercially available (Interferon Sciences or HydroMed Sciences). As an alternative, we employed Poly (ethylene glycol) Diacrylate (PEGDA) hydrogel as a substrate which releases VEGF into the corneal stroma in a manner analogous to the hydron/sucralfate pellets normally used. 6 kDa PEGDA was dissolved in a 10% solution with HBS. The photoinitiator 2,2-dimethoxy-2-phenylacetophenone was combined with N-vinylpyrrolidone (NVP) (300 mg/mL) and added to the polymer solution at a concentration of 10 μL/mL. The solution was vortexed and filter sterilized. PEGDA hydrogels were polymerized between two glass sides separated by a 0.005 inch thick poly(tetra fluoroethylene) (PTFE) spacer. The glass slides and spacer were secured using binder clips. VEGF (Sigma V7259) was mixed into the polymer solution to create a concentration of 320

ng VEGF per gel. 0.15 μL polymer solution was inserted in between glass slides using a Hamilton syringe and exposed to UV light (B-200SP UV lamp, UVP, 365 nm, 10 mW/cm^2) for two minutes. After exposure to UV light, crosslinked hydrogels were immediately inserted into the cornea micropocket.

Cornea Micropocket Angiogenic Assay

The micropocket assay was performed, with minor modifications, as previously described (Rogers et al., 2007). Mice were anesthetized with Avertin (0.2 ml/10 g body weight of a 1.25% solution) injected intraperitoneally (IP). The mice were placed on a heated Deltaphase Isothermal Pad (Braintree Scientific) to maintain body temperature at 37° C. The eye was topically anesthetized with one drop of 0.5% proparacaine (Bausch and Lomb). A partial-thickness incision in the mid-cornea was made followed by insertion of a von Graef knife to lengthen the pocket while pushing it toward the inferior limbus. Using a #5 forceps, VEGF-releasing hydrogels were then implanted within the pocket. Bacitracin zinc/ polymyxin B sulfate antibiotic ointment (Bausch and Lomb) was then applied to the eye and the mouse placed in a fresh cage on top of a heated pad for recovery from the anesthesia. Animals were sacrificed 6 days post-hydrogel implantation and the corneas processed into flat mounts for confocal analysis.

Supplementary Material

Refer to Web version on PubMed Central for supplementary material.

Acknowledgments

We would like to thank Katherine Fewell for superb technical assistance. We also thank members of the Dickinson lab for critical reading of this manuscript. This study was supported by The National Institute of Health (T32EY07102 and T32HD055200 to R.A.P. and R01HL077187, R01EB005173-01/05 and P20EB007076 to M.E.D.) and the American Heart Association (0625187Y to I.V.L.)

REFERENCES

Ambati BK, Nozaki M, Singh N, Takeda A, Jani PD, Suthar T, Albuquerque RJ, Richter E, Sakurai E, Newcomb MT, Kleinman ME, Caldwell RB, Lin Q, Ogura Y, Orecchia A, Samuelson DA, Agnew DW, St Leger J, Green WR, Mahasreshti PJ, Curiel DT, Kwan D, Marsh H, Ikeda S, Leiper LJ, Collinson JM, Bogdanovich S, Khurana TS, Shibuya M, Baldwin ME, Ferrara N, Gerber HP, De Falco S, Witta J, Baffi JZ, Raisler BJ, Ambati J. Corneal avascularity is due to soluble VEGF receptor-1. Nature. 2006; 443:993–997. [PubMed: 17051153]

Bani-Yaghoub M, Tremblay RG, Lei JX, Zhang D, Zurakowski B, Sandhu JK, Smith B, Ribecco-Lutkiewicz M, Kennedy J, Walker PR, Sikorska M. Role of Sox2 in the development of the mouse neocortex. Dev Biol. 2006; 295:52–66. [PubMed: 16631155]

Beebe DC. Maintaining transparency: a review of the developmental physiology and pathophysiology of two avascular tissues. Semin Cell Dev Biol. 2008; 19:125–133. [PubMed: 17920963]

Campochiaro PA, Hackett SF. Ocular neovascularization: a valuable model system. Oncogene. 2003; 22:6537–6548. [PubMed: 14528278]

Chan-Ling TL, Halasz P, Stone J. Development of retinal vasculature in the cat: processes and mechanisms. Curr Eye Res. 1990; 9:459–478. [PubMed: 2166637]

Diez-Roux G, Argilla M, Makarenkova H, Ko K, Lang RA. Macrophages kill capillary cells in G1 phase of the cell cycle during programmed vascular regression. Development. 1999; 126:2141–2147. [PubMed: 10207139]

Diez-Roux G, Lang RA. Macrophages induce apoptosis in normal cells in vivo. Development. 1997; 124:3633–3638. [PubMed: 9342055]

Dorrell MI, Aguilar E, Friedlander M. Retinal vascular development is mediated by endothelial filopodia, a preexisting astrocytic template and specific R-cadherin adhesion. Invest Ophthalmol Vis Sci. 2002; 43:3500–3510. [PubMed: 12407162]

Dyer MA, Farrington SM, Mohn D, Munday JR, Baron MH. Indian hedgehog activates hematopoiesis and vasculogenesis and can respecify prospective neurectodermal cell fate in the mouse embryo. Development. 2001; 128:1717–1730. [PubMed: 11311154]

Friedlander M. Fibrosis and diseases of the eye. J Clin Invest. 2007; 117:576–586. [PubMed: 17332885]

Fruttiger M. Development of the mouse retinal vasculature: angiogenesis versus vasculogenesis. Invest Ophthalmol Vis Sci. 2002; 43:522–527. [PubMed: 11818400]

Fruttiger M. Development of the retinal vasculature. Angiogenesis. 2007; 10:77–88. [PubMed: 17322966]

Gariano RF. Cellular mechanisms in retinal vascular development. Prog Retin Eye Res. 2003; 22:295–306. [PubMed: 12852488]

Gariano RF, Gardner TW. Retinal angiogenesis in development and disease. Nature. 2005; 438:960–966. [PubMed: 16355161]

Gimbrone MA Jr, Cotran RS, Leapman SB, Folkman J. Tumor growth and neovascularization: an experimental model using the rabbit cornea. J Natl Cancer Inst. 1974; 52:413–427. [PubMed: 4816003]

Gimbrone MA Jr, Leapman SB, Cotran RS, Folkman J. Tumor angiogenesis: iris neovascularization at a distance from experimental intraocular tumors. J Natl Cancer Inst. 1973; 50:219–228. [PubMed: 4692862]

Gimenez E, Montoliu L. A simple polymerase chain reaction assay for genotyping the retinal degeneration mutation (Pdeb(rd1)) in FVB/N-derived transgenic mice. Lab Anim. 2001; 35:153–156. [PubMed: 11315164]

Goldberg MF. Persistent fetal vasculature (PFV): an integrated interpretation of signs and symptoms associated with persistent hyperplastic primary vitreous (PHPV). LIV Edward Jackson Memorial Lecture. Am J Ophthalmol. 1997; 124:587–626. [PubMed: 9372715]

Hasegawa T, McLeod DS, Prow T, Merges C, Grebe R, Lutty GA. Vascular precursors in developing human retina. Invest Ophthalmol Vis Sci. 2008; 49:2178–2192. [PubMed: 18436851]

Ito M, Yoshioka M. Regression of the hyaloid vessels and pupillary membrane of the mouse. Anat Embryol (Berl). 1999; 200:403–411. [PubMed: 10460477]

Kenyon BM, Voest EE, Chen CC, Flynn E, Folkman J, D'Amato RJ. A model of angiogenesis in the mouse cornea. Invest Ophthalmol Vis Sci. 1996; 37:1625–1632. [PubMed: 8675406]

Klein R, Klein BE, Linton KL. Prevalence of age-related maculopathy. The Beaver Dam Eye Study. Ophthalmology. 1992; 99:933–943. [PubMed: 1630784]

Komitova M, Eriksson PS. Sox-2 is expressed by neural progenitors and astroglia in the adult rat brain. Neurosci Lett. 2004; 369:24–27. [PubMed: 15380301]

Lang R, Lustig M, Francois F, Sellinger M, Plesken H. Apoptosis during macrophage-dependent ocular tissue remodelling. Development. 1994; 120:3395–3403. [PubMed: 7821211]

Lang RA, Bishop JM. Macrophages are required for cell death and tissue remodeling in the developing mouse eye. Cell. 1993; 74:453–462. [PubMed: 8348612]

Langham M. Observations on the growth of blood vessels into the cornea; application of a new experimental technique. Br J Ophthalmol. 1953; 37:210–222. [PubMed: 13032381]

Larina IV, Shen W, Kelly O, Hadjantonakis A-K, Baron M, Dickinson M. A membrane associated mCherry fluorescent reporter line for studying vascular remodeling and cardiac function during murine embryonic development. The Anatomical Record. in press.

Lobov IB, Rao S, Carroll TJ, Vallance JE, Ito M, Ondr JK, Kurup S, Glass DA, Patel MS, Shu W, Morrisey EE, McMahon AP, Karsenty G, Lang RA. WNT7b mediates macrophage-induced programmed cell death in patterning of the vasculature. Nature. 2005; 437:417–421. [PubMed: 16163358]

McLeod DS, Hasegawa T, Prow T, Merges C, Lutty G. The initial fetal human retinal vasculature develops by vasculogenesis. Dev Dyn. 2006; 235:3336–3347. [PubMed: 17061263]

Meeson A, Palmer M, Calfon M, Lang R. A relationship between apoptosis and flow during programmed capillary regression is revealed by vital analysis. Development. 1996; 122:3929–3938. [PubMed: 9012513]

Millauer B, Wizigmann-Voos S, Schnurch H, Martinez R, Moller NP, Risau W, Ullrich A. High affinity VEGF binding and developmental expression suggest Flk-1 as a major regulator of vasculogenesis and angiogenesis. Cell. 1993; 72:835–846. [PubMed: 7681362]

Muthukkaruppan V, Auerbach R. Angiogenesis in the mouse cornea. Science. 1979; 205:1416–1418. [PubMed: 472760]

Panda A, Vanathi M, Kumar A, Dash Y, Priya S. Corneal graft rejection. Surv Ophthalmol. 2007; 52:375–396. [PubMed: 17574064]

Ritter MR, Aguilar E, Banin E, Scheppke L, Uusitalo-Jarvinen H, Friedlander M. Three-dimensional in vivo imaging of the mouse intraocular vasculature during development and disease. Invest Ophthalmol Vis Sci. 2005; 46:3021–3026. [PubMed: 16123396]

Rogers MS, Birsner AE, D'Amato RJ. The mouse cornea micropocket angiogenesis assay. Nat Protoc. 2007; 2:2545–2550. [PubMed: 17947997]

Saint-Geniez M, D'Amore PA. Development and pathology of the hyaloid, choroidal and retinal vasculature. Int J Dev Biol. 2004; 48:1045–1058. [PubMed: 15558494]

Shaner NC, Steinbach PA, Tsien RY. A guide to choosing fluorescent proteins. Nat Methods. 2005; 2:905–909. [PubMed: 16299475]

Speier S, Nyqvist D, Cabrera O, Yu J, Molano RD, Pileggi A, Moede T, Kohler M, Wilbertz J, Leibiger B, Ricordi C, Leibiger IB, Caicedo A, Berggren PO. Noninvasive in vivo imaging of pancreatic islet cell biology. Nat Med. 2008; 14:574–578. [PubMed: 18327249]

Yamaguchi TP, Dumont DJ, Conlon RA, Breitman ML, Rossant J. flk-1, an flt-related receptor tyrosine kinase is an early marker for endothelial cell precursors. Development. 1993; 118:489–498. [PubMed: 8223275]

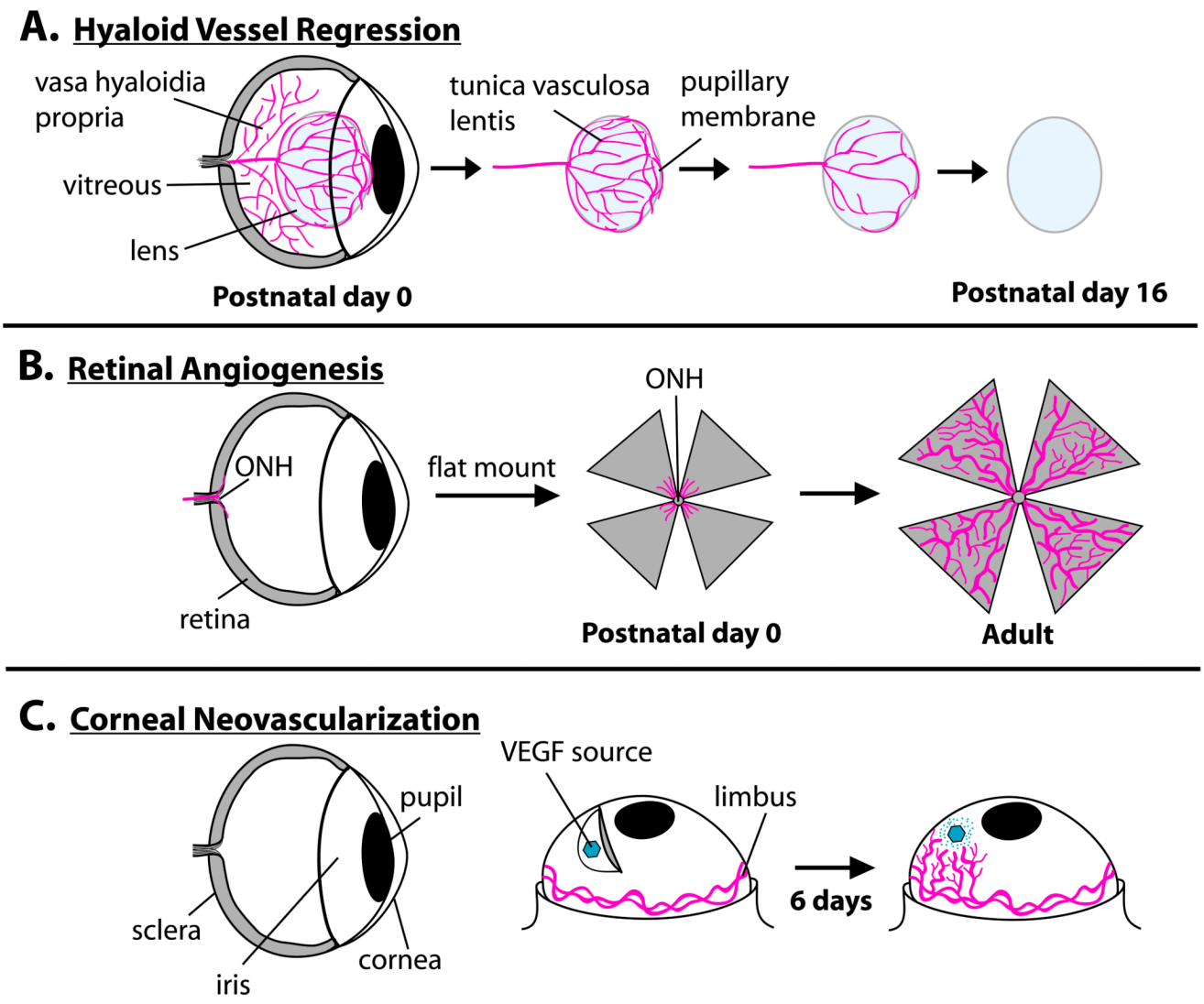

Figure 1. The three ocular vessel systems analyzed in this study

Hyaloid vessel regression, via apoptosis, begins immediately after birth. By postnatal day 16, a fully avascular lens is present **(A)**. Concurrently, retinal vessels begin to sprout out of the optic nerve head (OHN) and over the surface of the retina. By postnatal day 8, the primary vascular plexus has reached the retinal periphery **(B)**. Subsequently, the primary plexus branches into the retinal plexiform layers (not shown). The cornea is a normally avascular structure. By performing the corneal micropocket assay, one can supply the corneal stroma with a source of VEGF or other angiogenic factors and observe the process of neovascularization over time **(C)**.

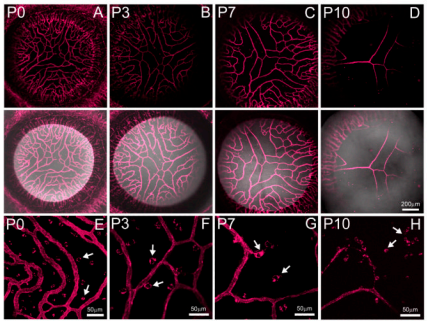

Figure 2. Flk1-myr::mCherry robustly labels the regressing pupillary membrane (PM) vessels *in vivo*

At P0, the extensive network of PM vessels is observed in live mice imaged by confocal analysis **(A)**. By P3, one begins to observe regression of the shorter vessel branches while the longer ones persist **(B)**. This pattern of regression is more obvious at P7 **(C)**. By P10, only the longest PM vessels remain **(D)**. Total PM elimination is observed by postnatal day 16 (data not shown) while the vessels of the developing iris persist. The lower panels of A–D show a myr::mCherry/brightfield merge. At higher magnification, discrete myr::mCherry + structures located outside of the vessel walls were observed **(E–H)**. These structures are further characterized in figure 3. In this and all subsequent figures, a minimum of three mice were examined at each age. Objectives used: Zeiss EC Plan-Neofluar 10×/0.3 NA and Zeiss Plan-Apochromat 20×/0.75 NA.

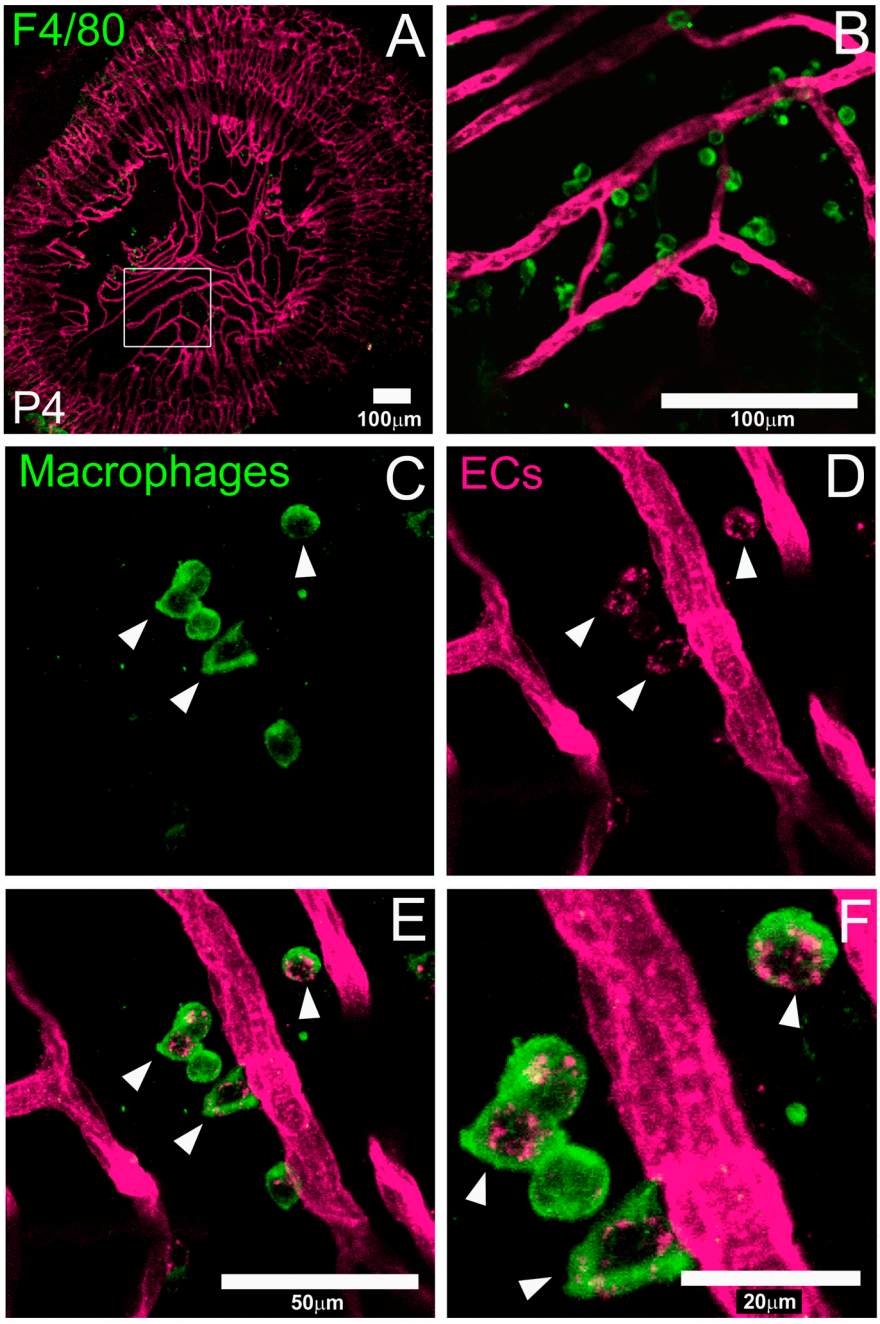

Figure 3. Flk1-myr::mCherry labels macrophage-engulfed endothelial cell (EC) debris

An antibody against F4/80 labels macrophages within the PM flat mount. Panels **A** and **B** are presented from low to high magnification in which the boxed region in **A** corresponds to panel **B**. At 40× magnification, we observed single macrophages most of which contain Flk1-myr::mCherry+ puncta **(arrowheads in C–F)**. This expression pattern suggests that the mCherry+ signal is coming from EC debris which has been engulfed by the macrophages. Objectives used: Zeiss Plan-Apochromat 20×/0.75 NA and Zeiss C-Apochromat 40×/1.2 NA.

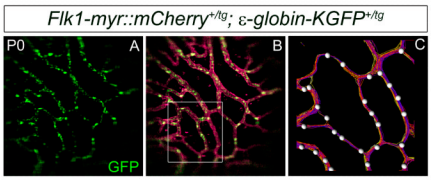

Figure 4. *Flk1-myr::mCherry*$^{+/tg}$; *ε-globin-KGFP*$^{+/tg}$ mice are useful for monitoring postnatal vessel hemodynamics

Shown here is a single frame taken from movie of GFP+ blood cells **(A)** flowing through the P0 myr::mCherry+ PM vasculature **(B)**. The box is meant to illustrate a region of interest where we applied the Imaris cell tracking software **(B)**. An enlargement of the area is provided to give a pictorial representation (single movie frame) of the cell tracking data. Here, individual cells are labeled with white spheres and tracks are represented by colored lines in which the color of an individual track changes over time **(C)**. Movies corresponding to these images are provided as supplementary data. Objective used: Zeiss Plan-Apochromat 20×/0.75 NA

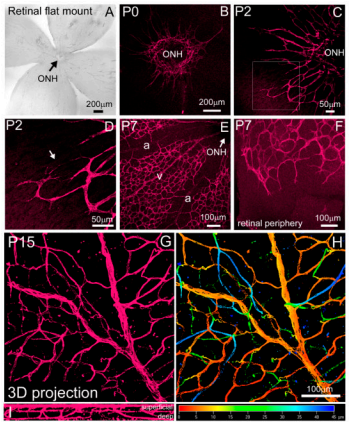

Figure 5. Flk1-myr::mCherry labels the earliest stages of retinal vessel development to full differentiation

Fixed retinal flat mounts were created for all time points indicated and imaged at the level of the nerve fiber layer **(A)**. At P0, myr::mCherry labeled the first vascular sprouts exiting the optic nerve head (ONH) **(B)**. Two days later, extension of the primary vascular plexus away from the ONH was apparent **(C)** and higher magnification revealed individual EC branching at the vascular front **(arrow in D)**. By P7, distinct arterial (a) and venous (v) differentiation was observed **(E)** and the vascular front extended toward the retinal periphery **(F)**. By P15, the primary and deep vascular plexuses have fully formed and was imaged through the entire depth of the retina **(G and I)**. By applying the depth coding function provided by the Zeiss LSM 510 software, the three-dimensional projection is color coded from the most superficial, primary plexus (red) to the deeper plexuses within the retina plexiform layers (blue) **(H)**. Images taken at 63X, revealed mature retinal vessels containing red blood cells (RBCs) **(I–K)**. Objectives used: Zeiss Plan-Apochromat 20×/0.75 NA and Zeiss EC Plan-Neofluar 10×/0.3 NA.

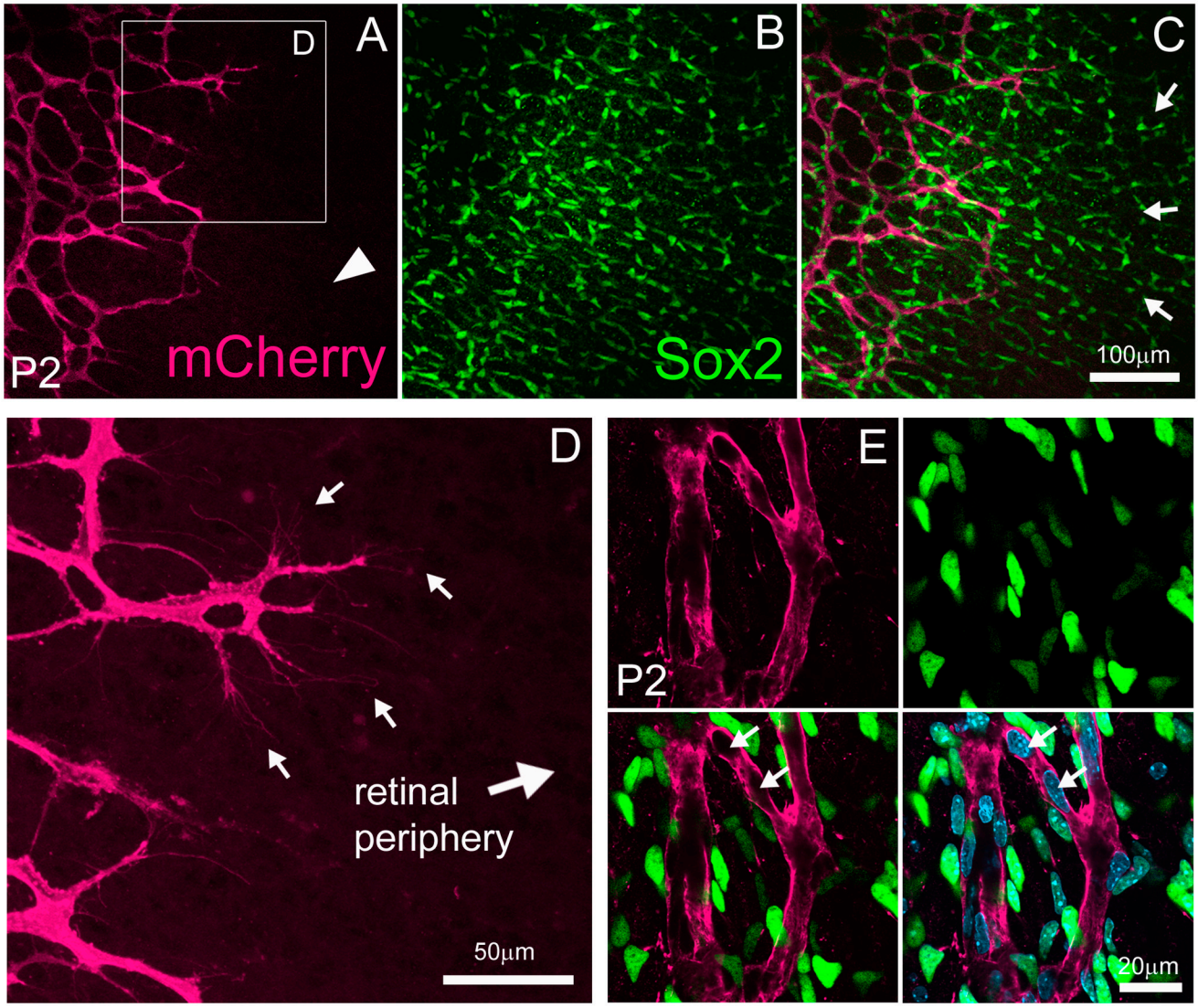

Figure 6. Flk1-myr::mCherry expression is consistent with an angiogenic model of retinal vascularization

By labeling P2 Flk1-myr::mCherry retinae with an antibody against Sox2, retinal astrocytes were seen ahead of the vascular front which was devoid of myr::mCherry+ cells **(arrowhead in A, B and arrows in C)**. Higher magnification imaging, revealed elaborate endothelial tip cell branching within the astrocyte template toward the retinal periphery **(arrows in D)**. Flk1-myr::mCherry, Sox2 and DAPI colocalization studies confirmed that myr::mCherry+ vessels are indeed negative for Sox2+ nuclei **(arrows in E)** thereby supporting a model of retinal angiogenesis (see text for details). Objectives used: Zeiss Plan-Apochromat 20×/0.75 NA, Zeiss C-Apochromat 40×/1.2 NA and Zeiss Plan-Apochromat 63×/1.4.

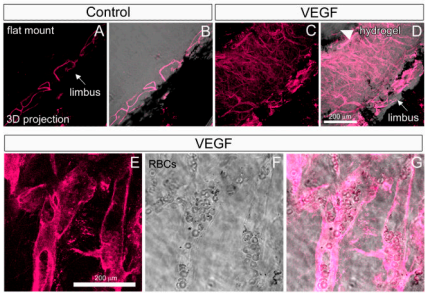

Figure 7. *Flk1-myr::mCherry*$^{+/tg}$ mice are a high-resolution reporter for adult corneal neovascularization

VEGF-induced corneal neovascularization was imaged by creating corneal flat mounts. **(A–D)**. In control samples, adult limbic vessels **(arrow in A and B)** normally do not enter the corneal stroma. In the presence of a local supply of VEGF implanted into the stroma (arrowhead in D), limbic vessel neovascularization into the cornea is observed 6 days post-implantation **(C and arrow in D)**. These vessels are easily detected by myr::mCherry expression. VEGF-induced neovessels were observed to contain RBCs suggesting lumen formation **(E–G)**. Objectives used: Zeiss Plan-Apochromat 20×/0.75 NA and Zeiss C-Apochromat 40×/1.2 NA.